Computational Techniques for Quantification and Optimization of Mixing in Microfluidic Devices

George Mathew, Linda Petzold *
Department of Mechanical and Environmental Engineering
University of California
Santa Barbara, CA 93106

Radu Serban †
Center for Applied Scientific Computing
Lawrence Livermore National Laboratory
Livermore, CA 94551

July 2, 2002

Abstract

In this paper we present computational techniques for quantifying and optimizing mixing in microfluidic devices. Theoretically, the mixing problem is very complex and unwieldy; therefore we develop computational tools which are as general as possible and which can potentially be applied to various micro-mixing devices. The availabilty of faster computers and the micro-scale nature of MEMS (Micro Electro Mechanical Systems) devices make it feasible to simulate numerous trajectories of tracer particles along the fluid flow and also to numerically optimize mixing.

1 Introduction

In this paper we present computational techniques for quantifying and optimizing mixing in microfluidic devices. The techniques described here are quite general. They can be applied in the case where there is a known (or previously computed) flow profile and the two fluids to be mixed have the same properties. The measures for mixing discussed here are robust and the computational techniques are efficient even though the underlying differential equations exhibit chaotic behaviour.

To illustrate our ideas, we consider a particular active mixing strategy for a micro-mixer developed by Volpert et al. [1] The active micro-mixing device is shown in Figure 1. It consists of a main mixing channel and three pairs of transverse secondary channels. The flow in the main channel is perturbed by a time-dependent transverse flow from the secondary channels, thereby enhancing mixing. Two unmixed fluids, one at the upper half and the other at the lower half, enter the main channel and are then manipulated by pressure-driven flow from the secondary channels. The two fluids referred to here are not two fluids with different properties, but can rather be thought of as the same fluid with different colored tracer particles in them. This mixing strategy is based on the principle of chaotic advection. Aref [2] and Ottino [3] have studied the use of chaotic advection to enhance mixing in laminar flows. Chaotic advection is the exponential separation of two adjacent particles over a period of time. Based upon this fundamental theoretical work, many researchers have attempted different approaches to micromixing. Optimization of mixing from a maximum entropy approach has been theoretically studied by D'Alessandro et al. in [6]. However, their study does not refer to any structure in the incoming fluid and therefore cannot be directly applied to our problem.

For the purposes of our study, a simple analytical flow based upon the superposition of elementary velocity profiles was assumed. The flow in the main channel follows a parabolic profile in the horizontal direction. The flow from the secondary channels consists of a vertical velocity with a parabolic profile that varies sinusoidally in time at different frequencies. It has been shown by Volpert et al. [1] that the mixing performace approximated by this simple analytical model qualitatively agrees with that obtained by a full

*This work was supported by NSF ACI-0086061 and University of Illinois PACI Subaward #814.

†The work of this author was performed under the auspices of the U.S. Department of Energy by the University of California, Lawrence Livermore National Laboratory under contract No. W-7405-Eng-48.

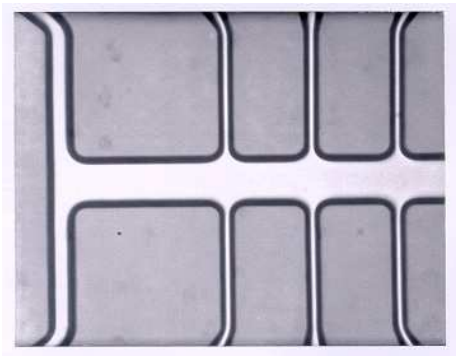

Figure 1: Micro-mixer device (device fabrication courtesy of K.S. Breuer, Brown University and R. Bayt, United Technologies)

Navier-Stokes simulation or Stokes simulation for low Reynolds numbers. However, it is not at all necessary for our computations described here to assume an analytical form for the flow field; they could just as well be found by a flow calculation. This micro-mixer has also been built and studied experimentally [7].

In this analysis, diffusion is neglected and mixing is assumed to be dependent only on the dynamics of the fluid interface. Mixing is caused by the efficient stretching and folding of the fluid interface. For a detailed study of mixing from this viewpoint, see [3]. Our objectives are to define and compute appropriate measures of mixing and to find the frequencies of the oscillating flow in the secondary channels which yield optimum mixing. For optimization, we make use of an optimization method which does not require derivatives, via the software package APPSPACK[4].

2 Mixer Geometry and Models

The micro-mixer is divided into three types of regions: the main channel (horizontal), the secondary channels (vertical), and the intersection regions. The dimensions of the mixer are as shown in Figure 2. A characteristic dimension of the mixer device is h, which is the half-width of the main channel where $h = 100\mu m$. In all our discussions, the origin of the $x - y$ plane is assumed to be at the center of the inlet.

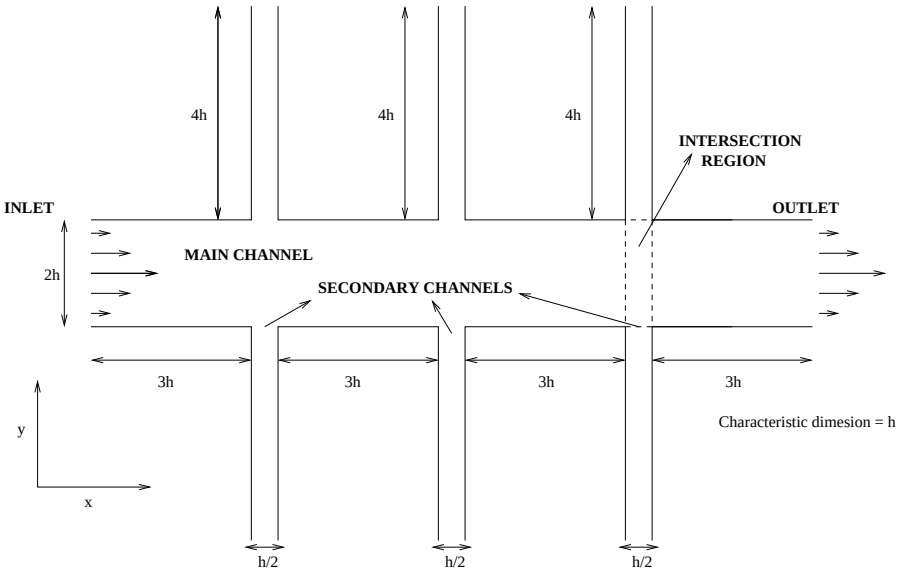

Figure 2: Dimensions of micro-mixer device

In this work, we assume a certain velocity vector field for the fluid over the entire mixer and study the resulting dynamics. In the main channel, fluid moves with a steady horizontal velocity ($\dot{x}$) which is parabolic in space. The horizonal velocity ($\dot{x}$) is zero outside the main channel. Two different optimization problems arise as a result of specifiying two different types of flow in the secondary channels. In the first, the maximum displacement is constant and the maximum velocity varies with the parameter (frequency). In the second, the maximum velocity is constant and the maximum displacement varies with the parameter (frequency). We refer to the first as Model I and the second as Model II. The vertical velocity ($\dot{y}$) is zero in regions of the main channel where it doesn't intersect with the transverse channels. In the intersection regions, the two above-mentioned velocity fields are superimposed. The velocity vector field is defined below. $\dot{x}$ refers to velocity in the x direction and $\dot{y}_i$ $(i = 1, 2, 3)$ refers to velocity in the y direction in the i^{th} secondary channel. The parameters are the frequencies f_i $(i = 1, 2, 3)$. The mixing efficiency and its variation with the parameters (pump frequencies) are interestingly different for both models.

2.1 Model I

$$\dot{x} = \begin{cases} 1 - (\frac{y}{h})^2, & -h \leq y \leq +h \\ 0, & y < -h,\ y > +h \end{cases} \tag{1}$$

$$\dot{y}_i = 4\pi f_i h \left[1 - \left(\frac{4\bar{x}}{h}\right)^2\right] \sin(2\pi f_i t), \tag{2}$$

where $\bar{x} = (3.5i - 0.25)h$ for $i = 1, 2, 3$.

2.2 Model II

$$\dot{x} = \begin{cases} 1 - (\frac{y}{h})^2, & -h \leq y \leq +h \\ 0, & y < -h,\ y > +h \end{cases} \tag{3}$$

$$\dot{y}_i = 4\pi h \left[1 - \left(\frac{4\bar{x}}{h}\right)^2\right] \sin(2\pi f_i t), \tag{4}$$

where $\bar{x} = (3.5i - 0.25)h$ for $i = 1, 2, 3$.

The scaling constant $4\pi h$ is introduced so that displacement along the centerline of the secondary channel is always $2h$ in the case for Model I and is $2h$ in the case for Model II only when the frequency is one.

3 Initial Approaches

We made several initial attempts to quantify the amount of mixing. These methods met with mixed success, but help to motivate the backward particle simulation method to be described in the next section. An interesting idea due to Meiburg [8] was to simulate the demarcation line between the two entering fluids. Theoretically, the demarcation line will never self-intersect, even after exiting the mixer. The motivation behind such a simulation was the one-dimensional aspect of the demarcation line, thereby giving the intuition that a lot of computational effort could be saved. The more space-filling the final perturbed demarcation line at the outlet of the mixer is, the more mixed the fluids should be. If the space after the mixer outlet was gridded in the horizontal and vertical directions, then the mixing measure will be a function of the arc lengths in each grid box. The objective function should be such that the sum of arc lengths in all grid boxes is maximized. This can be seen as a measure of the amount of stretching and folding the fluid interface went through. The problem with this approach is that it is almost impossible to numerically trace the demarcation line because of the extremely high sensitivities of the particle trajectories. Even though we could trace the demarcation line for the device with one pump, this approach drastically failed for the 3-pump case. In retrospect this is easily explained. It is characteristic of chaotic flows to not be able to numerically trace fluid interfaces.

Another approach, which we refer to as the 'forward particle simulation method', was originally employed by Volpert et al. [1] and consists of integrating the paths of many particles that are introduced at different positions and times at the inlet of the mixer. After a simulation of as many particles as possible, we collect final data for each particle $k = 1, 2, ..., N$ as a pair (t_k, y_k) which gives the time at which the particle reached the outlet and the vertical position at which the particle emerged from the mixer. Then the mixing is measured quantitatively in terms of the *mixing variance coefficient* which was introduced in [1]. Each particle is given a label based on its 'color': $l_k = 1$ for 'blue' particles (particles introduced in the upper half of the main channel) and $l_k = 0$ for 'red' particles (particles introduced in the lower half of the main channel). The channel exit is divided into S regions. At a given time t^*, the density of each region, ρ_i, is estmated by averaging the labels over the particles contained in that region during a specific time interval ΔT (centered at t^*)

$$\rho_i = \frac{\sum_{k=1}^{N_i} l_k}{N_i}, \tag{5}$$

where N_i is the number of particles contained in the i^{th} region. The *mixing variance coefficient* is then estimated by averaging over the S regions,

$$\Phi = \frac{1}{S}\sum_{i=1}^{S}(\rho_i - 0.5)^2. \tag{6}$$

For no mixing, $\Phi = 0.25$. For perfect mixing, $\Phi = 0$, corresponding to $\rho = 0.5$ in every region. The number of regions, S, defines the spatial scale at which the mixing is observed.

Problems with this approach

- The *mixing variance coefficient* defined in (6) is not even continuous with respect to the position of the particles. Our ultimate goal is to optimize the amount of mixing with respect to variation of the device parameters. The lack of continuity makes this objective unsuitable for use in a gradient-based optimizer. Even if a derivative-free optimizer were to be used, the lack of continuity of the objective function will affect the convergence and accuracy of results.
- The S regions chosen are non-overlapping. This can give inaccurate estimations of mixing. For instance, if the size of each region is very small and if each region has a density of 0 or 1, then the estimated mixing will be 0.25 while actually the mixing is good.
- By doing a 'forward simulation', we are forced to estimate mixing only in regions where a sufficient number of simulated particles ended up. Thus, we have no control over the time-space domain within which we want to estimate the mixing performance.

All of these problems are overcome by our approach, which we refer to as the 'backward particle simulation method', and also by defining the *mixing variance coefficient* more rigorously.

4 Simulation, Mixing Measures and Optimization

4.1 Backward Particle Simulation Method

In the 'backward particle simulation method' we fix a certain number of equally spaced particles in the vertical direction at the outlet of the mixer at several fixed times across a given time domain and then simulate the particle trajectories backward in time. Therefore, all we need to compute is the vertical position of each particle when it was at the inlet of the mixer. In other words, we compute the 'colour' of each particle. The justification for this approach is that the flow is volume-preserving and therefore we have constant particle density everywhere. Also, this is much more computationally efficient than the 'forward particle simulation method' because we are simulating only those particles within the space-time domain in which we are interested.

4.2 The Time-Averaged One Dimensional Mixing Variance Coefficient

Let $c(y)$ be the concentration distribution at the outlet of the mixer at a given time instant, where $y \in [a, b]$ and a and b are the lower and upper extremes of the region at the outlet within which we want to quantify mixing. $c(y)$ can be thought of as the limit of the concentration of blue (or red) fluid within intervals centered around y, as the size of the intervals go to zero. $d(p, s)$ is the average concentration in the interval $[p, p + s]$

$$d(p,s) = \frac{\int_p^{p+s} c(y)dy}{s}. \tag{7}$$

We define the *mixing variance coefficient at scale s* by

$$\phi_{1d}(s) = \frac{\int_a^{b-s} (d(p,s) - 0.5)^2 dp}{(b-a) - s}. \tag{8}$$

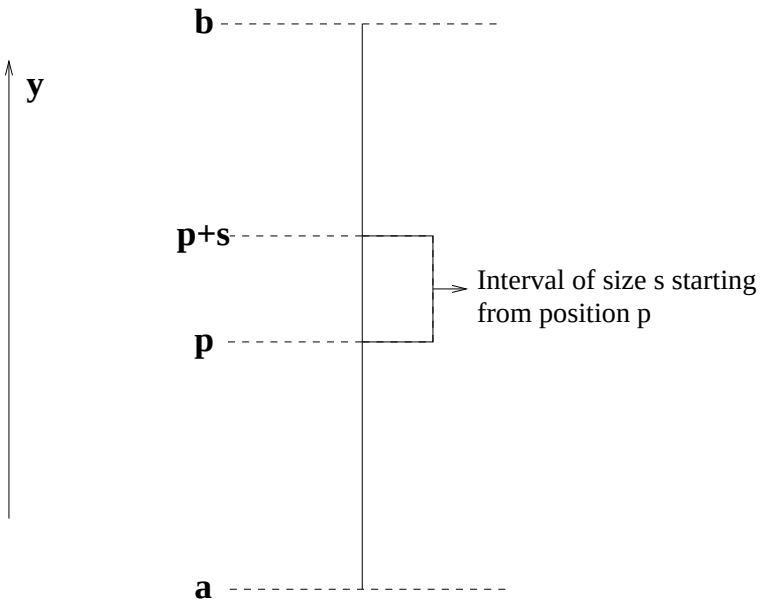

Figure 3: Illustration of the evaluation of the *mixing variance coefficient at scale s*. $d(p, s)$ is evaluated by integrating $c(y)$ within the interval shown in the figure and dividing by s. $\phi_{1d}(s)$ is evaluated by sliding the interval shown in the figure from a to $b - s$ and evaluating the integral of $(d(p, s) - 0.5)^2$ and diving by $(b-a)-s$. The global mixing variance coefficient is the average of $\phi_{1d}(s)$ over all possible scales $s \in [0, b-a]$.

Note that

$$\lim_{s \to 0} d(p,s) = c(p),$$

and therefore

$$\lim_{s \to 0} \phi_{1d}(s) = \frac{\int_a^b (c(p) - 0.5)^2 dp}{(b-a)}.$$

Similarly,

$$\lim_{s \to (b-a)} \phi_{1d}(s) = \left(\frac{\int_a^b c(p)dp}{(b-a)} - 0.5 \right)^2.$$

Thus $\phi_{1d}(s)$ is well-defined for all $s \in [0, b-a]$. We define the *global mixing variance coefficient* by

$$\Phi_{1d} = \frac{\int_0^{b-a} \phi_{1d}(s)ds}{(b-a)}. \tag{9}$$

For perfect mixing, if we choose an interval of any size and location along the outlet, we should get an average concentration of 0.5. Therefore, closeness to perfect mixing for a given concentration distribution can be estimated only by defining the *global mixing variance coefficient* as shown above. In other words, Φ_{1d} is the mean square deviation of the average concentration over intervals of all possible sizes at all possible locations along the outlet of the mixer. For the case $c(y) = 0 \quad or \quad 1$ for all $y \in [a, b]$, $\Phi_{1d} = 0.25$ indicating the worst mixing possible. This corresponds to the case when there is only one fluid along the outlet. For the case $c(y) = 0.5$ for all $y \in [a, b]$, $\Phi_{1d} = 0$ indicating perfect mixing. The method by which $\phi_{1d}(s)$ can be estimated is discussed in the next section. The final objective functoin is Φ_{1d} averaged over a given time domain.

4.2.1 Computation of the One Dimensional Mixing Variance Coefficient

For our computation with the backward simulation method of the mixing in the micro-mixing device of Figure 1, we place N equally spaced particles along the outlet vertically at a given time t^*. Let the spacing between adjacent particles be $dy = \frac{(b-a)}{(N-1)}$ and let the particles be indexed by subscript i $(i = 0, 1, 2, ...(N-1))$. Then the vertical position of particle i at the outlet is given by $y_i = a + idy$. The position of each particle when it was at the inlet is obtained by a backward simulation in time. Let yin_i be the position of particle i when it was at the inlet. Let $yin(y)$ be the resulting linearly interpolated function which is a map from the outlet vertical position to the inlet vertical position. Then the concentration distribution at the outlet can be approximated by

$$\hat{c}(y) = \begin{cases} 1 & \text{if } yin(y) > 0 \\ 0 & \text{if } yin(y) < 0. \end{cases} \tag{10}$$

Thus the average concentration in the interval $[y_p, y_{p+n}]$ is estimated by

$$\hat{d}(y_p, y_{p+n}) = \frac{\sum_{i=p}^{p+n-1} I(y_i, y_{i+1})}{n}, \tag{11}$$

where

$$I(y_i, y_{i+1}) = \begin{cases} 1 & \text{if } yin_i \times yin_{i+1} > 0 \text{ and } yin_i > 0 \\ 0 & \text{if } yin_i \times yin_{i+1} > 0 \text{ and } yin_i < 0 \\ \frac{yin_{i+1}}{(yin_{i+1} - yin_i)} & \text{if } yin_i \times yin_{i+1} < 0 \text{ and } yin_i < 0 \\ \frac{yin_i}{(yin_i - yin_{i+1})} & \text{if } yin_i \times yin_{i+1} < 0 \text{ and } yin_i > 0 \end{cases} \tag{12}$$

The *mixing variance coefficient at scale* $s_n = n \times dy$ is estimated by

$$\hat{\phi}_{1d}(s_n) = \frac{\sum_{p=0}^{N-n-1} (\hat{d}(y_p, y_{p+n}) - 0.5)^2}{(N-n)}. \tag{13}$$

The *global mixing variance coefficient* can be estimated by

$$\hat{\Phi}_{1d} = \frac{0.25 + \sum_{n=1}^{N-1} \hat{\phi}_{1d}(s_n)}{N}, \tag{14}$$

where $s_n = n \times dy$ and $\hat{\phi}_{1d}(s_i)$ is computed using (13).

We note that $\hat{\phi}_{1d}(s)$ will be a poor estimate for $\phi_{1d}(s)$ if n and N are not chosen appropriately. Thus we need to perform convergence tests and find the n and N at which $\hat{\phi}_{1d}(s)$ converges. Once we fix s and n, $N = (n-1)\frac{(b-a)}{s} + 1$. In the following experiment we fix $s = 0.1$ and vary n to study convergence. We set $a = -0.9h$ and $b = 0.9h$. This is just to avoid having to integrate paths of particles which are very close to the wall and which don't affect the mixing computations much because of the low percentage of fluid which is flowing through the neglected regions due to the low velocities there. All the pump frequencies were set to one and the *mixing variance coeffcient at scale* $s = 0.1$ was computed for ten different time snapshots across a time domain of one unit and averaged. Figure 4 shows the variation of $\hat{\phi}_{1d}(s)$ with respect to n for different numbers of pumps. Let n_c be the n at which $\hat{\phi}_{1d}(s)$ converges. Clearly, as the number of pumps

increases, n_c increases. Roughly speaking, dy is the scale within which $yin(y)$ can be approximated by an affine function. Figure 5 shows the variation of $\hat{\Phi}_{1d}$ with respect to N for different numbers of pumps. As the number of pumps increases the curves in Figure 4 and Figure 5 become more noisy, which is expected because the flow becomes more chaotic. Figure 6 shows the variation of $\hat{\phi}_{1d}(s)$ with respect to s. As s approaches $(b-a)$, $\hat{\phi}_{1d}(s)$ approaches almost zero. As s approaches zero, $\hat{\phi}_{1d}(s)$ approaches 0.25.

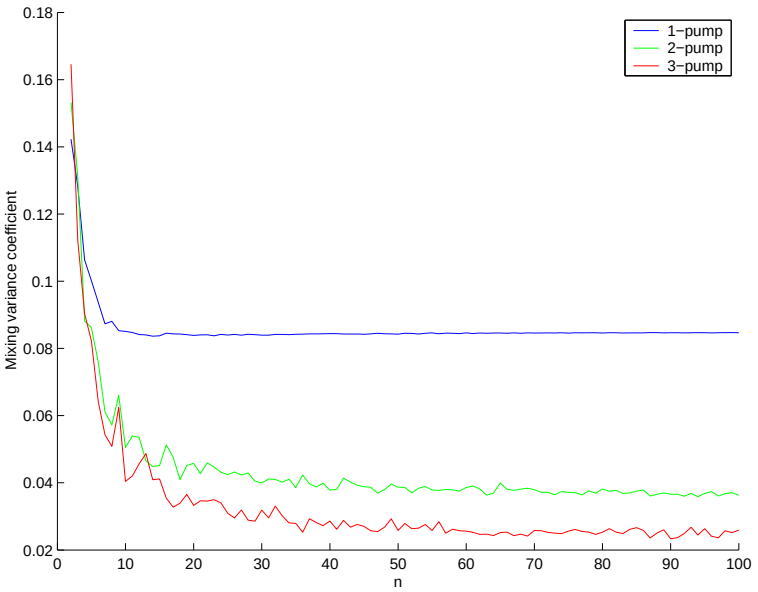

Figure 4: Variation of $\hat{\phi}_{1d}(s)$ for $s = 0.1$ with respect to n for different numbers of pumps

4.2.2 Optimization

It is feasible to do a brute-force search for the optimum parameters when there is only one pump. Figure 7 shows the variation of the *global mixing variance coefficient* with respect to the parameter for both Model I and Model II with just one pump. Figure 8 shows the variation of the *mixing variance coefficient at scales* $s = 0.1$ *and* $s = 0.05$. It is interesting to observe that the *global mixing variance coefficient* varies almost periodically with respect to the parameter in the case of Model I, whereas in the case of Model II there is only one minimum and at high frequencies we get very poor mixing. In fact, the minimum occurs when the frequency is around one, which is when the displacement along the centerline of the secondary channel is exactly the width of the main channel.

Another interesting question is whether the optimum frequency for mixing will be independent of the numbers of pumps if all pumps have the same frequency. Figures 9 and 10 suggest that this is indeed true. This is an unexpected and useful result because it says that no matter how many pumps you have, if all the pumps have the same frequencies then you need only to optimize for the 1-pump case.

A brute-force search becomes impractical in the case of 2 or 3 pumps. Therefore we must employ optimization software. We decided against using a gradient-based optimizer because of the non-smooth velocity profile, the high cost for sensitivity computations and the high sensitivity of the particle trajectories to the parameters. Therefore our attention was directed to direct search methods that do not use derivatives, but only objective function values. Pattern search methods, which form a subset of direct search methods, are very effective for optimization problems with no constraints, few parameters and very expensive objective function evaluations, such as the problem at hand. We used the Asynchronous Parallel Pattern Search (APPS) software developed by T.G. Kolda et al. [4] at Sandia National Laboratories. The optimization algorithm is parallelized. The essence of the optimization algorithm is the pattern of search directions which drive the search. Parallelism is achieved by dividing the search directions among the different processors. For a convergence analysis of pattern search methods see [5].

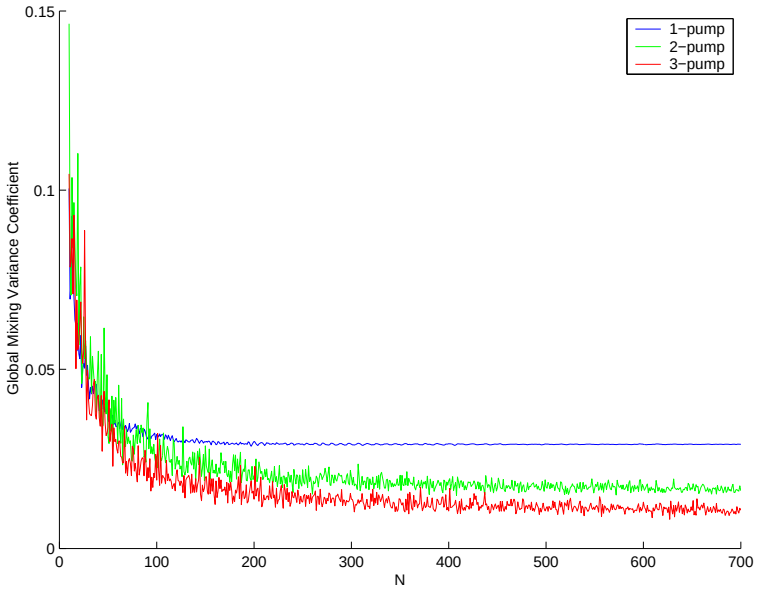

Figure 5: Variation of $\hat{\Phi}_{1d}$ with respect to N for different numbers of pumps

Shampine and Gordon's solver for nonstiff initial value problems in ordinary differential equation systems [9] was used for the particle simulations. In the following optimization experiments, the parameters for the 'backward particule simulations' with reference to Section 4.2.1 are $s = 0.05$, $n = 20$, $a = -0.9h$; $b = 0.9h$, absolute tolerance for the ODE solver $= 10^{-7}$, and relative tolerance for the ODE solver $= 10^{-7}$.

The *mixing variance coefficient at scale s* was computed for ten equally spaced time snapshots from 0 to 1 and averaged to get the final objective function. All the optimization computations were done on a Beowulf cluster of 42 Linux based workstations. APPS requires $2P + 2$ number of processors where P is the number of optimization parameters [1]. The parameters given to APPS were initial step length $= 1.0$, minimum step length $= 0.0002$, and convergence tolerance $= 10^{-4}$.

Results for Model I with one pump

- Optimal mixing measure, $\phi(s) = 0.09513187$;
- Optimum frequency, $f_1 = 1.167603$;
- Number of iterations $= 11$;

Results for Model II with one pump

- Optimal mixing measure, $\phi(s) = 0.1174625$;
- Optimum frequency, $f_1 = 1.062622$;
- Number of iterations $= 4$;

These results agree with the optimum values as seen in Figure 8, thereby demonstrating the effectiveness of APPS for this problem.

[1] It should be possible to parallelize over the trajectory computations as well as over the optimization parameters, but we have not implemented that.

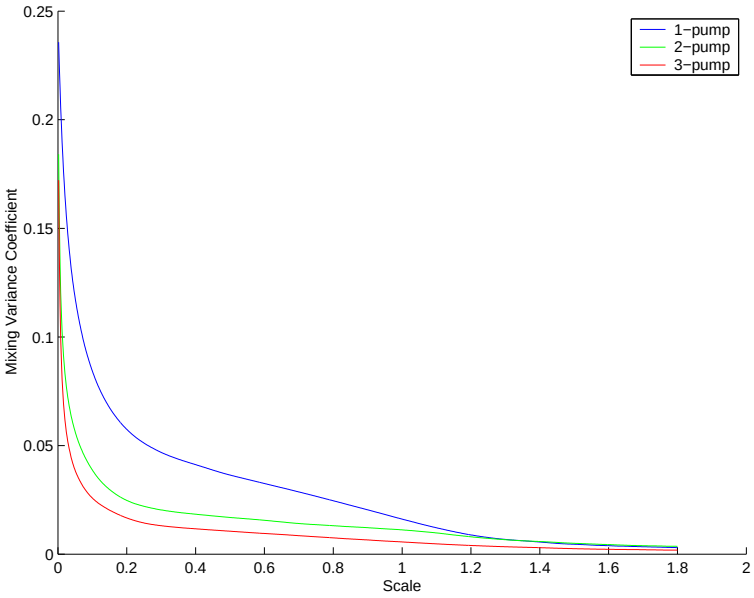

Figure 6: Variation of $\hat{\phi}_{1d}(s)$ with respect to s for different numbers of pumps

Results for Model I with three pumps

- Optimal mixing measure, $\phi(s) = 0.01422374$;
- Optimum frequencies, $f_1 = 1.063232$, $f_2 = 2.283203$, $f_3 = 3.0$;
- Number of iterations = 15;

Results for Model II with three pumps

- Optimal mixing measure, $\phi(s) = 0.01737651$;
- Optimum frequencies, $f_1 = 1.0$, $f_2 = 1.0$, $f_3 = 1.936523$;
- Number of iterations = 10;

We note that there are many local minima for this problem and therefore APPS could be converging to one of these local minima. Thus, optimum values obtained from APPS are sensitive to the parameters like initial step length. Nevertheless it was observed that the optimal mixing measures obtained from different optimization runs were comparable.

4.3 The Two Dimensional Mixing Variance Coefficient in the Time-Space Domain

The mixing measure Φ_{1d} discussed in Section 4.2 is appropriate for situations where strong mixing is required in the vertical direction and mixing in the horizontal direction is not so important. This section describes a more general version of the *mixing variance coefficient*. In general, the final objective function will depend on the actual engineering application and how the fluid from the outlet is utilized. But the spirit of all of these measures is essentially the same.

Let $c(t, y)$ be the concentration distribution in the time-space domain at the outlet of the mixer where $(t, y) \in [t_0, t_f] \times [a, b]$ which is the time-space domain within which we want to quantify mixing. $d(p_t, p_y, s_t, s_y)$ is the average concentration in the rectangle whose corners are (p_t, p_y) and $(p_t + s_t, p_y + s_y)$

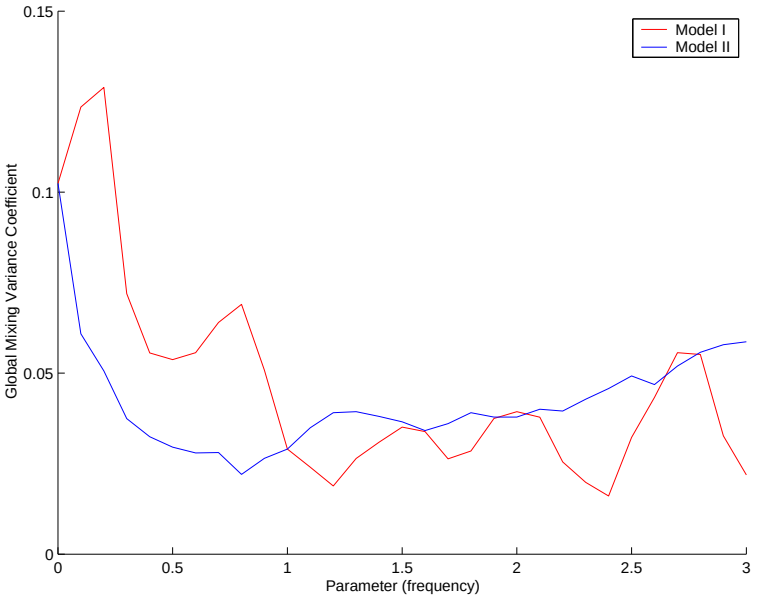

Figure 7: Variation of the *global mixing variance coefficient* with respect to the parameter for both Model I and Model II with one pump

$$d(p_t, p_y, s_t, s_y) = \frac{\int_{p_y}^{p_y+s_y} \int_{p_t}^{p_t+s_t} c(t,y)dtdy}{s_y \times s_t}. \tag{15}$$

We define the *mixing variance coefficient at scale '$s_t \times s_y$'* by

$$\phi(s_t, s_y) = \frac{\int_a^{b-s_y} \int_{t_0}^{t_f-s_t} (d(p_t, p_y, s_t, s_y) - 0.5)^2 dp_t dp_y}{(t_f - t_0 - s_t) \times (b - a - s_y)} \tag{16}$$

$\phi(s_t, s_y)$ is well-defined for all $(s_t, s_y) \in [0, t_f - t_0] \times [0, b-a]$. We define the *global mixing variance coefficient* by

$$\Phi = \frac{\int_0^{b-a} \int_0^{t_f-t_0} \phi(s_t, s_y) ds_t ds_y}{(t_f - t_0) \times (b - a)}. \tag{17}$$

In short, the *global mixing variance coefficient* is the mean square deviation of the average concentration over all open rectangles within the time-space domain of interest. There is no reason for defining it likewise other than for computational ease. The same could have been defined over all open spheres which is probably a better choice or possibly over all connected sets. But the computation becomes non-trivial in those cases and more theory is required regarding such measures. Note that $\phi(0, s_y) = \phi_{1d}(s_y)$.

4.3.1 Computation of the Two Dimensional Mixing Variance Coefficient in the Time-Space Domain

For our computation with the backward simulation of the mixing in the micro-mixing device, we place N_y equally spaced particles along the outlet vertically at N_t equally spaced time snapshots ranging from t_0 to t_f. Let the spacing between adjacent particles in the vertical direction be $dy = \frac{(b-a)}{(N_y-1)}$ and the spacing between adjacent particles in the time direction be $dt = \frac{(t_f-t_0)}{(N_t-1)}$. Let the particles be indexed by subscripts (i, j). Let $t_i = t_0 + idt$ and $y_j = a + jdy$. In the time-space domain, the coordinates of particle (i, j) are (t_i, y_j). The position of each particle when it was at the inlet is obtained by a backward simulation in time. Let $yin_{i,j}$ be the position of particle (i, j) when it was at the inlet. Let $yin(t, y)$ be the resulting linearly

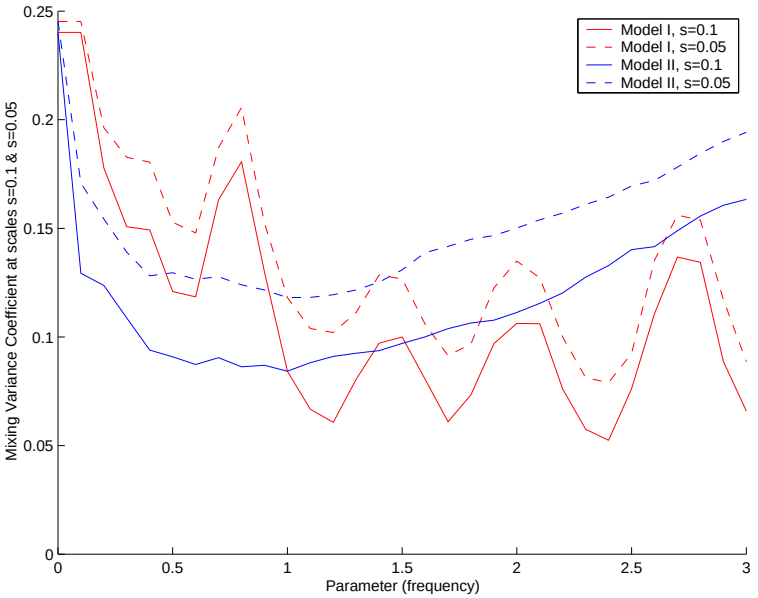

Figure 8: Variation of the *mixing variance coefficient at scales* $s = 0.1$ *and* $s = 0.05$ with respect to the parameter for both Model I and Model II with one pump

interpolated function which is a map from the time-space domain at the outlet to the inlet vertical position. Then the concentration distribution in the time-space domain at the outlet can be approximated by

$$\hat{c}(t,y) = \begin{cases} 1 & \text{if } yin(t,y) > 0 \\ 0 & \text{if } yin(t,y) < 0. \end{cases} \tag{18}$$

Thus the average concentration in the rectangle whose corners are (t_p, y_q) and (t_{p+n_t}, y_{q+n_y}) with $n_t, n_y > 1$ is estimated by

$$\hat{d}(t_p, y_q, t_{p+n_t}, y_{q+n_y}) = \frac{\sum_{j=q}^{q+n_y-1} \sum_{i=p}^{p+n_t-1} I(t_i, y_j, t_{i+1}, y_{j+1})}{n_t \times n_y}, \tag{19}$$

where

$$I(t_i, y_j, t_{i+1}, y_{j+1}) = I1(i,j) + I2(i,j). \tag{20}$$

$I1(i,j)$ is the ratio of the area in the triangle with vertices $[(t_i, y_j), (t_{i+1}, y_j), (t_{i+1}, y_{j+1})]$ for which $yin(t,y) > 0$ and $I2(i,j)$ is the ratio of the area in the triangle with vertices $[(t_i, y_j), (t_i, y_{j+1}), (t_{i+1}, y_{j+1})]$ for which $yin(t,y) > 0$. $\hat{d}(t_p, y_q, t_p, y_{q+n_y})$ is given by (11) and $\hat{d}(t_p, y_q, t_{p+n_t}, y_q)$ is given by something similar to (11) but applied in the time direction. Also, $\hat{d}(t_p, y_q, t_p, y_p) = 0.25$.

The *mixing variance coefficient at scale* '$s_{n_t} \times s_{n_y}$' where $s_{n_t} = n_t dt$ and $s_{n_y} = n_y dy$ is estimated by

$$\hat{\phi}(s_{n_t}, s_{n_y}) = \frac{\sum_{q=0}^{N_y-n_y-1} \sum_{p=0}^{N_t-n_t-1} (\hat{d}(t_p, y_q, t_{p+n_t}, y_{q+n_y}) - 0.5)^2}{(N_t - n_t) \times (N_y - n_y)}. \tag{21}$$

The *global mixing variance coefficient* is estimated by

$$\hat{\Phi} = \frac{\sum_{n_y=0}^{N_y-1} \sum_{n_t=0}^{N_t-1} \hat{\phi}(s_{n_t}, s_{n_y})}{N_t \times N_y}, \tag{22}$$

where $s_{n_t} = n_t dt$ and $s_{n_y} = n_y dy$ and $\hat{\phi}(s_{n_t}, s_{n_y})$ is computed using (21).

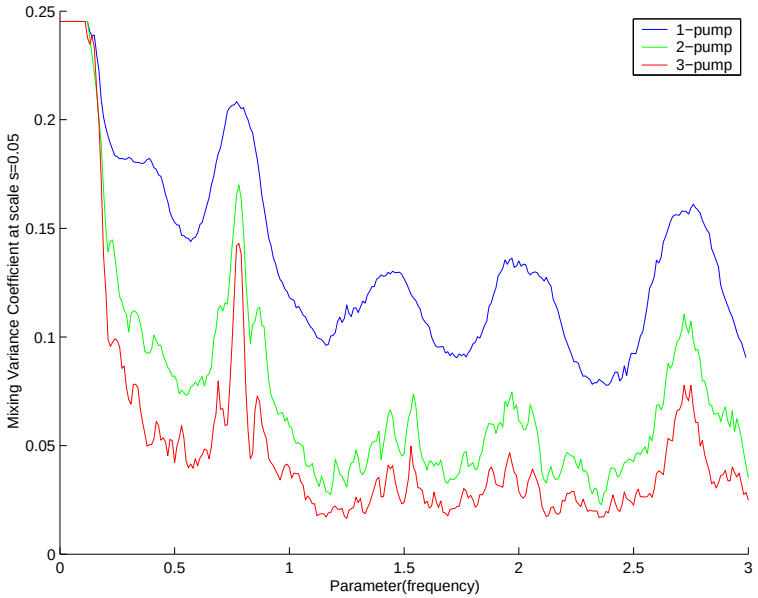

Figure 9: Variation of the *mixing variance coefficient at scale* $s = 0.05$ with respect to the parameter (frequency) for Model I with different numbers of pumps when all of the pumps have the same frequency

Note: The computational complexity for computing $\hat{\Phi}$ can be immense if $\hat{d}(t_p, y_q, t_{p+n_t}, y_{q+n_y})$ for $n_t, n_y > 1$ is computed directly using (19). Therefore the following relation is exploited when computing $\hat{\Phi}$.

$$\begin{aligned}\hat{D}(t_p, y_q, t_{p+n_t}, y_{q+n_y}) = \hat{D}(t_p, y_q, t_{p+n_t-1}, y_{q+n_y-1}) + \hat{D}(t_{p+n_t-1}, y_q, t_{p+n_t}, y_{q+n_y-1}) \\ + \hat{D}(t_p, y_{q+n_y-1}, t_{p+n_t-1}, y_{q+n_y}) + \hat{D}(t_{p+n_t-1}, y_{q+n_y-1}, t_{p+n_t}, y_{q+n_y}),\end{aligned} \tag{23}$$

where $\hat{D}(t_p, y_q, t_{p+n_t}, y_{q+n_y}) = n_t n_y \hat{d}(t_p, y_q, t_{p+n_t}, y_{q+n_y})$.

Just as for the one-dimensional case, we need to perform convergence tests to find the N_y and N_t at which $\hat{\Phi}$ converges. In this experiment we set $a = -0.9h$, $b = 0.9h$, $t_0 = 0$ and $t_f = 1$. Also, we assume that N_y is equal to the N for which $\hat{\Phi}_{1d}$ converged. Figure 11 shows the variation of $\hat{\Phi}$ with respect to N_t for different numbers of pumps.

4.3.2 Optimization

The parameters for the computation of Φ with reference to Section 4.3.1 are $N_y = 250$, $N_t = 20$, $a = -0.9h$, $b = 0.9h$, $t_0 = 0$ and $t_f = 1$. Figures 12 and 13 show the variation of Φ with respect to the parameter for Model I and Model II respectively with different numbers of pumps when all of the pumps have the same frequency. The ODE solver, the optimization software and the parameters given to the optimization software were the same as in Section 4.2.2.

Results for Model I with one pump

- Optimal mixing measure, $\Phi = 0.006199652$;
- Optimum frequency, $f_1 = 1.148315$;
- Number of iterations = 9;

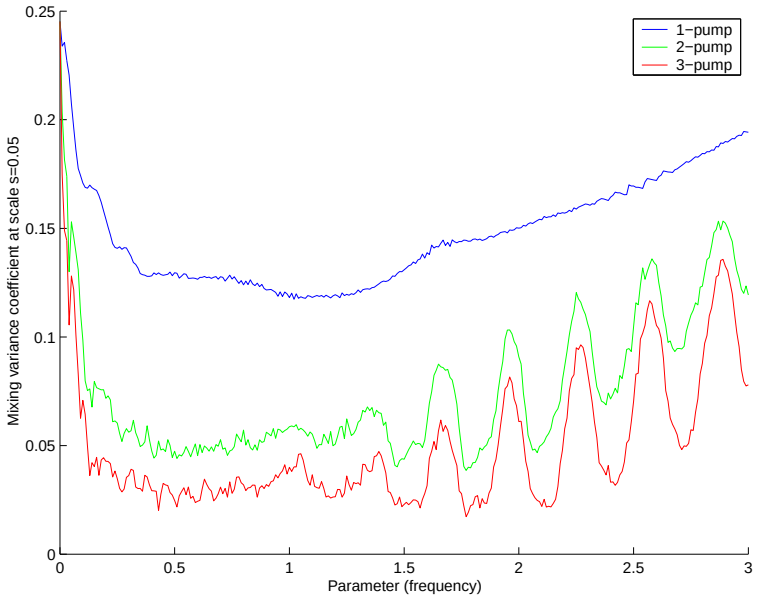

Figure 10: Variation of the *mixing variance coefficient at scale* $s = 0.05$ with respect to the parameter (frequency) for Model II with different numbers of pumps when all of the pumps have the same frequency

Results for Model II with one pump

- Optimal mixing measure, $\Phi = 0.009629172$;
- Optimum frequency, $f_1 = 0.59375$;
- Number of iterations = 5;

These results agree with the optimum values as seen in Figures 12 and 13.

Results for Model I with three pumps

- Optimal mixing measure, $\Phi = 0.001584305$;
- Optimum frequencies, $f_1 = 1.093450$, $f_2 = 0.02429199$, $f_3 = 1.250000$;
- Number of iterations = 21;

Results for Model II with three pumps

- Optimal mixing measure, $\Phi = 0.001461693$;
- Optimum frequencies, $f_1 = 0.9992676$, $f_2 = 1.003906$, $f_3 = 2.501953$;
- Number of iterations = 13;

5 Conclusions

We have introduced practical and physically meaningful measures for mixing via the *mixing variance coefficient at scale s* and the *global mixing variance coefficient*. We have presented the 'backward particle simulation method' for efficient computation of the mixing measures and also demonstrated the robustness of the mixing measure even though the underlying differential equations are chaotic. The mixing measures

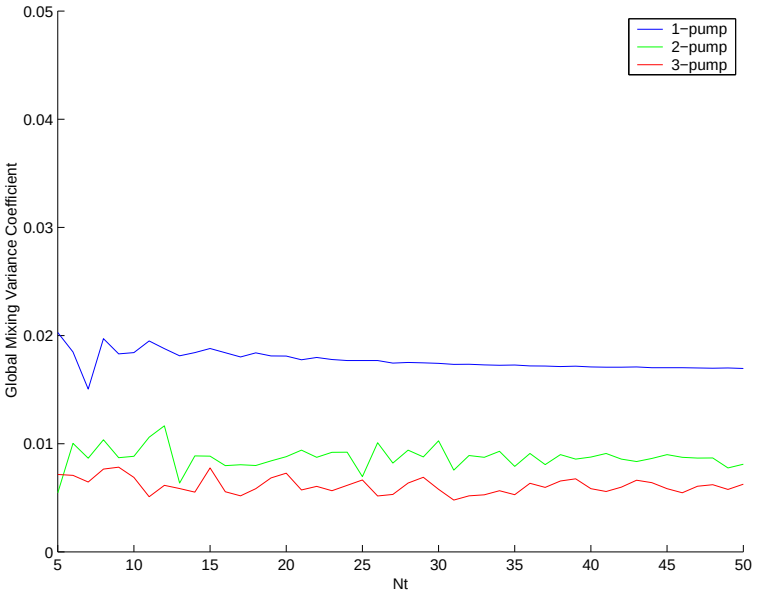

Figure 11: Variation of $\hat{\Phi}$ with respect to N_t for different numbers of pumps

introduced are tractable for optimization and we demonstrated that the optimization can be accomplished with pattern search methods.

Acknowledgments

The authors would like to thank Muruhan Rathinam and Igor Mezic for their helpful suggestions, and Carl Meinhart for information on the micromixing device.

References

[1] M. Volpert, C. D. Meinhart, I. Mezic and M. Dahleh, *Modeling and analysis of mixing in an actively controlled micromixer*, in preparation.

[2] H. Aref, *Stirring by chaotic advection*. Journal of Fluid Mechanics, 143, 1-21 (1984).

[3] J.M.Ottino, *The Kinematics of Mixing: Stretching, Chaos and Transport*. Cambridge University Press, Cambridge, England 1989.

[4] P.D.Hough, T.G.Kolda and V.Torczon, *Asynchronous Parallel Pattern Search for Nonlinear Optimization*. SIAM J. Scientific Computing 23(1):134-156, June 2001.

[5] V. Torczon, *On the Convergence of Pattern Search Algorithms*. SIAM Journal on Optimization, Volume 7, Number 1, pp.1-25.

[6] D'Alessandro, M. Dahleh and I. Mezic, *Control of Mixing: A Maximum Entropy Approach*. IEEE Transactions on Automatic Control 44(1999):1852-1864.

[7] N. Soundarrajan, *Flow Visualization of Mixing Processes in Microscale Geometries*. Masters thesis, Mechanical and Environmental Engineering, University of California, Santa Barbara, 2002.

[8] E. Meiburg, University of California, Santa Barbara, Personal Communication, 2001.

[9] L.F. Shampine and M.K. Gordon, *Computer Solution of Ordinary Differential Equations*. W. H. Freeman and Co., San Francisco, 1975.

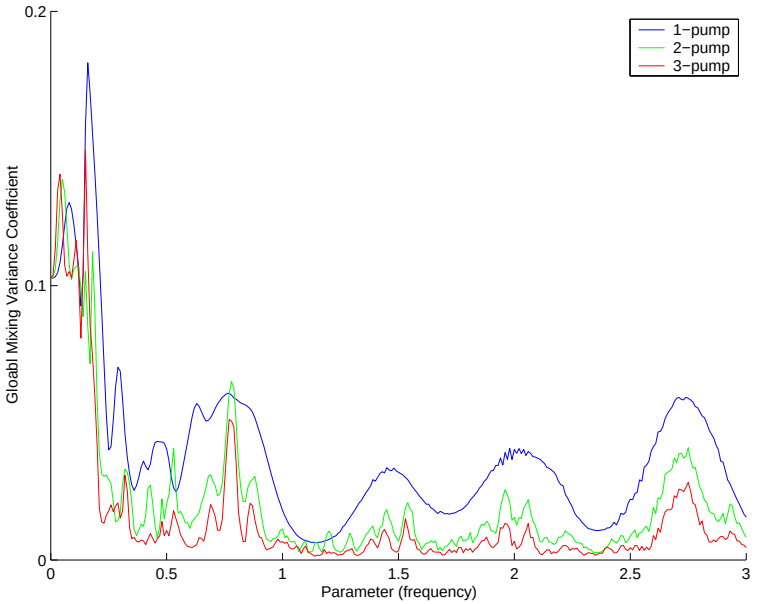

Figure 12: Variation of $\hat{\Phi}$ with respect to the parameter (frequency) for Model I with different numbers of pumps when all of the pumps have the same frequency

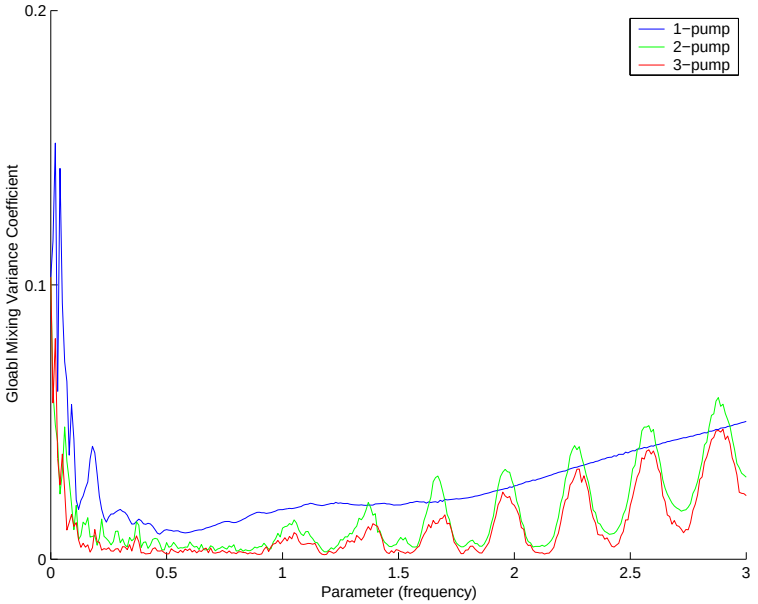

Figure 13: Variation of $\hat{\Phi}$ with respect to the parameter (frequency) for Model II with different numbers of pumps when all of the pumps have the same frequency